Journal of Hydrology: Regional Studies 47 (2023) 101372

Contents lists available at ScienceDirect

Journal of Hydrology: Regional Studies

journal homepage: www.elsevier.com/locate/ejrh

The combined impact of shallow groundwater and soil salinity on evapotranspiration using remote sensing in an agricultural alluvial setting

Hesham M. Aboelsoud [a], Ayman Habib [b], Bernard Engel [c], Ahmed A. Hashem [d,e,f], Waleed Abou El-Hassan [g,h], Ajit Govind [i], Abdelrazek Elnashar [j], Mona Eid [a], Ahmed M.S. Kheir [a,i,*]

[a] Soils, Water and Environment Research Institute, Agricultural Research Center, 9 Cairo University Street, Giza 12112, Egypt
[b] Lyles School of Civil Engineering, Purdue University, 550 Stadium Mall Drive, West Lafayette, IN 47907, USA
[c] Agricultural & Biological Engineering Department, Purdue University, 225 South University Street, West Lafayette, IN 47907, USA
[d] College of Agriculture, Arkansas State University, Jonesboro, AR 72467, USA
[e] Division of Agriculture, University of Arkansas System, Little Rock, AR 72204, USA
[f] Agricultural Engineering Department, Suez Canal University, Ismailia 41522, Egypt
[g] Water Management Research Institute, National Water Research Center, NWRC Building, 13621-5 Delta Barrage, Egypt
[h] FAO, Egypt, 11 Al Eslah El Zerai St., Dokki, PO. Box: 100, Cairo, Egypt
[i] International Center for Agricultural Research in the Dry Areas (ICARDA), Maadi 11728, Egypt
[j] Department of Natural Resources, Faculty of African Postgraduate Studies, Cairo University, Giza 12613, Egypt

ARTICLE INFO

Keywords:
Groundwater
Remote sensing
Crop water use
Arid regions
Eddy covariance
LANDSAT 8

ABSTRACT

Study region: The Nile Delta, Egypt
Study focus: Shallow groundwater (GW) and soil salinity are major issues for irrigated agriculture, particularly in arid and semi-arid regions, but more research is needed to link both issues with evapotranspiration. Satellite-based evapotranspiration from Landsat images (ET_{LS}) has the potential to be an efficient method of estimating evapotranspiration (ET), which can integrate ET_{LS} with groundwater and soil salinity, particularly in data-scarce areas. This study examines shallow GW and soil salinity effects on crop water use in the North Nile Delta during the summer season of 2017 and winter season of 2017/2018.
New hydrological insights for the region: The ET_{LS} was moderately affected by groundwater depth (GWD), decreasing from 4.3 to 4.0 mm day^{-1} when GWD was reduced from 75 to 120 cm, then increasing to 4.4 mm day^{-1} when GWD was increased to 140 cm. The study also highlighted a significant negative correlation between ET_{gw} and GWD; which increased with shallower GW (>75 cm) and then decreased with deeper GW. The shallower the GW, the greater the contribution to crop water requirements, with GW contributing 1.6 and 1.7 mm day^{-1} for seed melon and cotton, respectively, while GW contributed 0.9 mm day^{-1} for sugar beet and 1.3 mm day^{-1} for wheat and clover. The study's findings highlight the importance of remote sensing and GIS techniques for quickly and cheaply assessing the impact of shallow GW and soil salinity on evapotranspiration over large geographic areas.

* Correspondence to: Soils, Water & Environment Research Institute (SWERI), Agric. Res. Centre (ARC), Giza, Egypt.
E-mail addresses: ahmedkheir@arc.sci.eg, drahmedkheir2015@gmail.com (A.M.S. Kheir).

https://doi.org/10.1016/j.ejrh.2023.101372
Received 8 November 2022; Received in revised form 25 March 2023; Accepted 31 March 2023
Available online 7 April 2023

1. Introduction

Waterlogging and shallow groundwater (GW) have caused many environmental problems in many places worldwide due to poor irrigation and nonfunctional drainage systems, particularly with flood irrigation (Ochoa et al., 2007; Zhang et al., 2021). The groundwater depth (GWD) is often considered an essential factor in controlling ET rates (Devitt et al., 2002). Consequently, higher ET rates commonly occur with the shallowest *GW* and vice versa (Nichols, 1994). The relationship between ET and GWD, in general, is not straightforward, whereas a range of responses including a strong effect (Lafleur and Roulet, 1992), a moderate effect (Lafleur et al., 2005), or no significant effect of GWD has been observed (Wu et al., 2010), especially in peat-lands (Moore et al., 2013). This relationship is primarily influenced by several key factors, including soil hydraulic properties and soil matric potential at the root zone's long boundary. Furthermore, clay soils are vulnerable to drying and wetting cycles, which can cause cracks in the soil profile and macropore flow paths that rapidly deliver water, nutrients, and pollutants to the water table (Kurtzman and Scanlon, 2011). Although recent studies have explored the integration between remote sensing (RS) and surface and groundwater consumption in humid areas (Peña-arancibia et al., 2016), analysis of arid regions has not been performed yet. In addition to GWD, linear relationships were found between soil salinity and ET (Cemek et al., 2011). For instance, (Ünlükara et al., 2008) observed a decrease in ET of an okra due to soil salinity with a threshold value of 3.48 dS m^{-1}. In contrast, the formation of soil salt crusts results in reduced soil evaporation under constant meteorological conditions (Zhang et al., 2013), possibly due to the increase of soil albedo (Fujimaki et al., 2006). Elhaddad et al. (2007) found that ET values correlated well with soil salinity when they used GIS and RS techniques. Nonetheless, the integration of ET, GWD, and soil salinity using RS in arid regions needs more attention.

Irrigated agriculture faces several challenges that require special attention, such as natural soil salinity and groundwater (Ding et al., 2020a; Ding et al., 2020b), waterlogging, and water scarcity. The presence of saline groundwater in the North Nile Delta Aquifer as a result of seawater intrusion (Khatib, 1971; Mabrouk et al., 2019 and Ding et al., 2020). The injudicious use of poor quality groundwaters in many arid and semi-arid regions for irrigation leads to the build-up of salinity and/or sodicity in soil and deterioration of soil health (Jat et al., 2018). Therefore, (El-Ghannam et al., 2019) and (Ding et al., 2020) observed that the highest soil and groundwater salinity and sodicity values were recorded near the sea due to seawater intrusion. However, to achieve proper groundwater resource management in this region, it is necessary to determine the actual heterogeneity and stratigraphy of the Nile Delta aquifer to understand the patterns of seawater movement and mixing between fresh and saline groundwater (El-Kiki, 2018).

Shallow GW has long been recognised for its contribution to plant ET(Shah et al., 2007b). Whereas the decoupling of GW and root zone began at GWD 30–100 cm for deep-rooted vegetation, depending on soil texture (Shah et al., 2007a), and it can be used in-situ through its capillary rise (Dinar et al., 1991), especially as water becomes scarce (Shankar, 2012). With modified irrigation management, *GW* can cover part of or total crop ET (Logsdon et al., 2009) when it lies near the bottom of the root zone (Ayars et al., 2006). The contribution of GW may reduce or even eliminate irrigation requirements without compromising crop yields (Nosetto et al., 2009). However, the contribution of GW decreases with increasing irrigation applications (Karimov et al., 2014) and decreases by approximately 25% for every 1 m decline in the watertable(Xu et al., 2016). As a result, lowering the GW reduced the annual ET by about 32% and reduced ET_{gw} by about 62% (Cooper et al., 2006). Cordeiro et al. (2015) found that GW contributed 52–81% to crop ET depending on the GW depth; thus, maintaining the *GW* at a shallow depth was suggested to be desirable to the plants (Shouse et al., 2006). For instance, the contribution of GW within a 40–150 cm depth met more than 65% of seasonal wheat ET (Liu and Luo, 2011) and (Yang et al., 2007) 50% for alfalfa (Ayars et al., 2009), especially with proper irrigation management. Additionally, entire wheat, maize, sorghum ET, and 20% sunflower ET were covered from GW at a depth of 50 cm (Kahlown et al., 2005) due to the hydraulic connection between the unsaturated and saturated zones. Moreover, the capillary rise supplied 29% of wheat ET with a mean GWD of 1.5 m (Huo et al., 2012), 12–30% of soybean ET with 1.5–2.0 m *GWD* (Videla Mensegue et al., 2015), and 33–50% for corn and wheat with GWD of 0.5 and 2.5 m, respectively (Kang et al., 2001). GW can contribute to crop ET by up to 80% without affecting its yield and soil salinity (Prathapar and Qureshi, 1999a).

Plants' groundwater consumption is difficult to measure, although it is a critical factor of the water budget in arid and semi-arid environments (Loheide et al., 2005). Plants transpire water during the daylight hours by utilizing a portion from *GW*, so its depth decreases. Similarly, when transpiration significantly diminishes or ceases at night, the GW will rise due to lateral and vertical GW flow (McWhorter and Sunada, 1977). Consequently, diurnal GWD fluctuations, produced by diurnal fluctuations in plant ET (during the day and night times), can be used to measure GW contribution to crop ET. Hence, in temperate climates, one of the most important diurnal fluctuation-inducing factors for shallow GW is the water consumption of vegetation (Gribovszki et al., 2010). So, diurnal GW fluctuation methods to calculate ET and GW flow increase interest in ecohydrological studies (Mazur et al., 2014).

The ET during night time (ET_N) was 7% for the entire day (ET_{24}) for tall grass vegetation (Sugita and Brutsaert, 1991), 4.1% of ET_{24} for a willow tree (Iritz and Lindroth, 1994), and 14% of ET_{24} for alfalfa as the wind speed increased (Malek, 1992). Also, the ET_N proportion out of ET_{24} ranged from 3% for dry-land cotton to 7.2% for irrigated alfalfa (Tolk et al., 2006). On the other hand, Novick et al. (2009) found that plant stomata are closed at night, preventing ET, so ET_N averaged 8–9% of mean daytime ET (ET_D) is driven mainly by wind and vapor pressure deficit.

Finally, diurnal fluctuations in wetland water levels reflect direct GW uptake by plants, where they draw down water levels during daylight hours, and GW flows continuously, but its elevation mostly recovers at night, as GW flux replenishes the water extracted by ET (Loheide et al., 2009). However, this typical pattern of groundwater fluctuation cannot be applied in some conditions. For example, Cordeiro et al. (2015) determined the redistribution pattern of water in the effective root zone subjected to irrigation and GW contribution. They discovered that during periods of high ET demand, the soil grows drier, and during periods of low ET demand, the soil becomes wetter. Groundwater depth can become deeper and may have a delay in the drying/replenishment cycle during the night in poorly drained soils.

Nevertheless, to the best of our knowledge, no existing study has evaluated the effect of salinity and groundwater level on ET in arid regions using RS techniques. Therefore, the main objectives of this research were to 1) estimate ET_{LS} using Landsat satellite data, 2) evaluate the impact of GWD and soil salinity on ET_{LS}, and 3) evaluate the GW contribution to crop water consumption (ET_{gw}).

2. Materials and methods

2.1. Study site

The study was implemented in 200 ha of commercial fields in North Nile Delta, Egypt, during the summer season of 2017 and winter season of 2017/2018 to assess the impact of GWD on crop water consumption. The main cultivated crops were rice, cotton, maize, and seed melon in the summer growing season and wheat, clover, and sugar beet through the winter season. The area was divided into six parts, as shown in Fig. 1, according to salinity and GWD distribution. All parts in the area of study were planted with the same crops (Supplementary Table 1), and irrigated using fresh water through traditional surface flood irrigation.The area is located between 31° 14' and 31° 11'N and 30° 58' and 31° 01'E, so it is subjected to the same climate conditions. The mean daily temperature ranges between 4.9 and 35.1 °C, and the average annual precipitation is about 140 mm. The area has a subsurface drainage system installed at 2 m with 25 m lateral spacing. The GW ranged between 0.5 and 1.5 m below the ground surface. The area is generally salt-affected clayey soil, and its EC values vary from 4 to 10 dS m^{-1} with low hydraulic conductivity. Soil salinity (EC_e) was estimated using Ground Electro Magnetic Meter (EM_{38}). Soil chemical analysis was carried out to determine pH, water-soluble Ca^{2+}, Mg^{2+}, K^+, Na^+, Cl^-, HCO_3^- and SO_4^{2+}. In addition, soil physical analysis was carried out to identify soil particle distribution, water field capacity (FC), infiltration rate (IR), hydraulic conductivity (HC), and soil bulk density (BD). The chemical and physical analyses were carried out following (Black, 1965) and (Jackson, 1967), as shown in supplementary Tables 2 and 3. Soil salinity was evaluated using soil samples as well as the EM_{38} survey. According to Aboelsoud and Abdelrahman (2017), the EM_{38} -mk2 metre readings (EC_a) were converted to soil electrical conductivity (EC_e) by calibrating with augured soil samples from the same plots. Crop classifications for the two growing

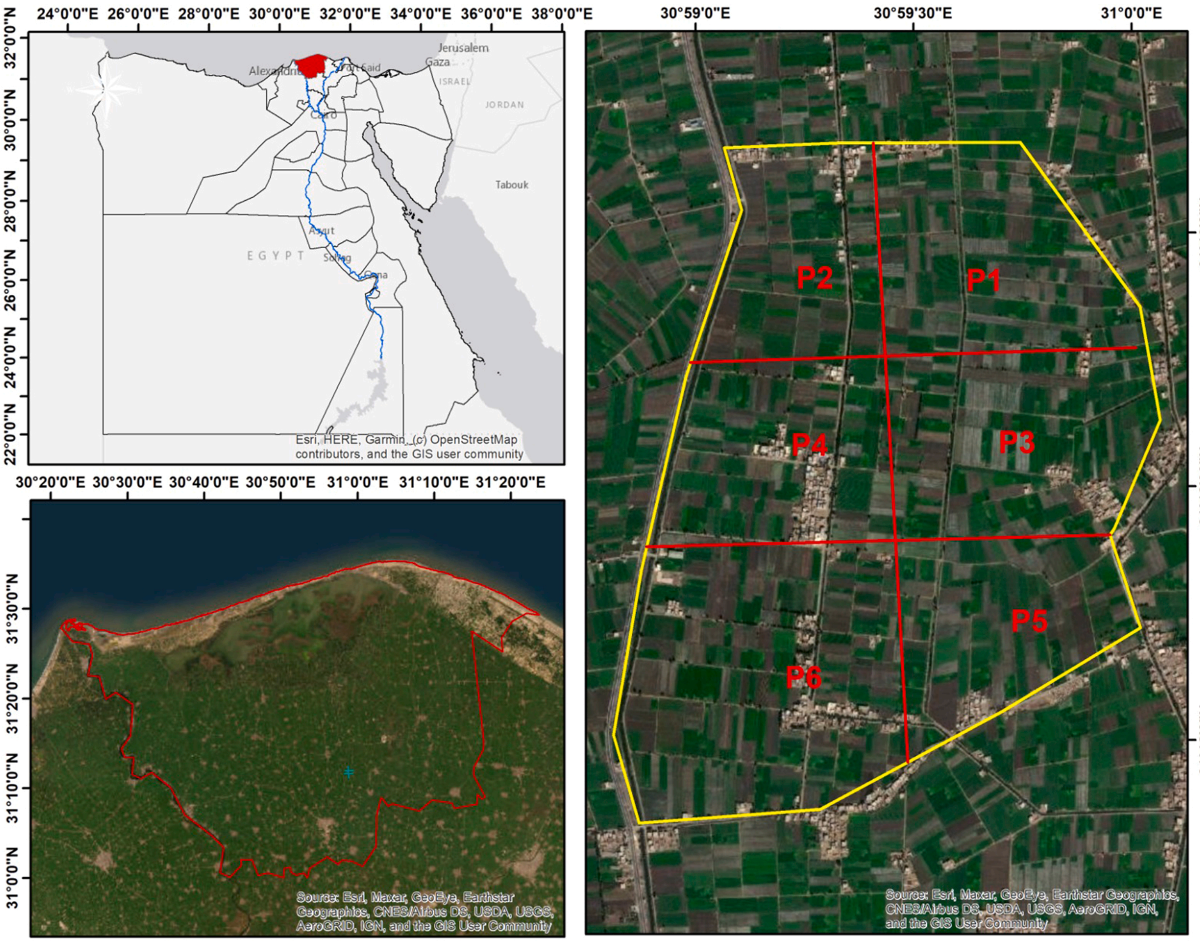

Fig. 1. The study area at Kafrelsheikh District, North Nile Delta (divided into six parts).

seasons were conducted, and the land use was extracted and identified using Landsat 8 satellite imagery (Campbell, 1996).

2.2. Evapotranspiration

2.2.1. Field-based evapotranspiration

Eddy covariance stations were used in the field for evapotranspiration measurements (ET_{EC}). It is a simple system and easy-to-use method for calculating ET (Moorhead et al., 2019). The $ET_{EC}$is a direct method for measuring the exchange between the atmosphere and surface in diverse environments, notwithstanding its flaws, particularly in terms of energy balance closure (Baldocchi, and Aubinet et al., 2014, 2012). Thus, it was used to validate remote sensing ET in several previous studies (e.g., Globally (Michel et al., 2016) Asia (Kim et al., 2012); South Africa (Majozi et al., 2017); Europe (Hu et al., 2015); North America (Mu et al., 2011); Europe and the United States (Miralles et al., 2011); the United States (Xu et al., 2019); and China (Li et al., 2018). The instruments were connected to a CR6 data recorder (Campbell Scientific), and measurements were recorded every six seconds. The data was then averaged or summed to provide 30-minute data.

2.2.2. Satellite-based evapotranspiration

Indirect estimation of the crop evapotranspiration from remote sensing using Landsat satellite images (Landsat 8: ET_{LS}) was achieved using the daily component of the energy balance equation:

$$Rn = G + H + \lambda E \tag{1}$$

Where Rn is the net radiation (Wm^{-2}), G is the soil heat flux (Wm^{-2}), H is the sensible heat flux (Wm^{-2}), and λE is the latent heat flux, which is associated with the actual ET (Wm^{-2}). The energy balance can be written as:

$$\lambda E = EF * (Rn - G) \tag{2}$$

Where EF is the dimensionless evaporative fraction, and Rn-G the net available energy for ET. G can often be ignored for time scales of 1 day, and thus λE is a function of Rn and EF only (Zwart et al., 2010). TheλE is also defined as the ratio of actual ET to the available energy.

$$EF = \frac{\lambda E}{Rn - G} \tag{3}$$

The Triangle method (Rasmussen Mads Olander et al., 2014) used in this study equation (Priestley and Taylor, 1972):

$$\lambda E = \phi\left[(Rn - G) \times \left(\frac{\Delta}{\Delta + \gamma}\right)\right] \tag{4}$$

Where ϕ is the psychometric constant ($kPa\,K^{-1}$), and substituted for the P–T parameter; and $\Delta$is the slope of saturated vapor pressure at the air temperature ($kPa\,K^{-1}$). The P–T parameter is assumed to be 1.26 for wetland surface conditions according to (Jiang and Islam, and Tang et al., 1999, 2010);(Arasteh and Tajrishy, 2008; Gan et al., 2020).

EF can be rewritten from Eqs. 5, 6 and 7 as follows:

$$EF = \frac{\lambda E}{Rn - G} = \phi\left(\frac{\Delta}{\Delta + \gamma}\right) \tag{5}$$

According to the Lijuan et al. (2016) approach, the Normalized Difference Vegetation Index (NDVI) and Land Surface Temperature

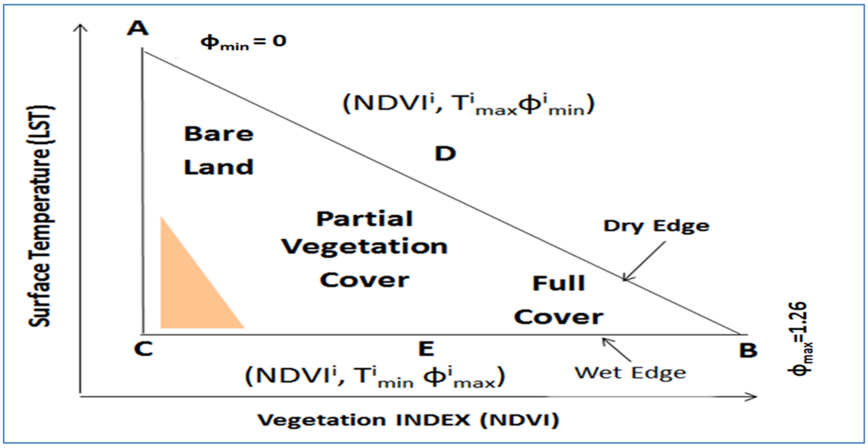

Fig. 2. Schematic diagram interpretation of the scatter plot of (LST–NDVI) triangular space to estimate evaporative fraction.

(LST) triangle method (Fig. 2) were applied to estimate the psychometric constant parameter. It originated from the parameterization of Jiang and Islam (1999) in a simplified Priestley-Taylor formula. Also, a spectral radiance model and a web-based atmospheric correction model can be used to successfully evaluate LST from thermal bands of Landsat data (Aboelnour and Engel, 2018). Regional ET_{LS} and *EF* were estimated according to Eq. 6, which depends on remotely sensed data. The accurate interpretation of the scatter plot resulting from remotely sensed LST and NDVI under variances in soil moisture availability, and vegetation cover leads to an accurate estimation of regional ET_{Ls}. The rate of ET is influenced by vegetation and restricted by soil moisture on the dry edge (as AC) of the triangular space, and the value of psychometric constant is the least under the same condition.

The Landsat 8 Operational Land Imager (OLI) data from July 2017 to June 2018 developed the triangular space (Table 1). The processed remote sensing data, including the NDVI and LST as radiometric calibration and atmospheric correction, were used as measured data. Statistical analysis was conducted, and the coefficient of determination (R^2), Root Mean Square Error (RMSE), Mean Bias Error (MBE), and Nash-Sutcliffe Efficiency (NSE) statistical parameters were estimated to validate the daily satellite-based ET_{LS} values compared to the ET_{EC}.

2.3. Groundwater depth

Groundwater positions were monitored in 18 observation wells (2-inch diameter PVC pipe) from July 2017 to June 2018. Automatic electronic pressure level logger sensors (Solinst Canada LT F30/M10, Model 3001) were installed in nine of these wells for automated recording of GWD at one-hour intervals (S.Fig. 1). Also, the GW diurnal cycle was determined. The fluctuations in GWD for day and night times were used to predict the contribution of GW to crop water use according to the methods described by (McWhorter and Sunada, 1977). Therefore, the average GWD during the daylight time (from sunrise to sunset) and nighttime (from sunset of a specific day to the sunrise of the following day) was calculated for each well. The differences between both were calculated for each month of the study period. The Solinst pressure sensors were submerged in the groundwater at 200 cm depth below the soil surface; therefore, they were not affected by air temperature fluctuations. There were no differences between day and night temperatures recorded by the sensors. For example, air temperature during June was 34^0 C in the daytime and 21^0 C in the nighttime, while the temperature recorded by the pressure sensors at the same time was 21.7^0 C during both day and night. On the other hand, the solinst logger readings were the atmospheric pressure plus the GW pressure on the sensors. A Solinst Baro-logger (Model 3001, CE LT F5/M1.5) was used to estimate the corrected GW by subtracting its reading from the readings of Solinst pressure sensors. Therefore, the effects of the atmospheric pressure fluctuations on sensor readings were removed. To calculate the ET_{gw} value, the drop in GWD measured in the monitoring wells was multiplied by the soil specific yield (~12%), which was calculated as the difference between the porosity and field capacity of the soil (Satchithanantham et al., 2014). The soil-specific yield is "the volume of water that an unconfined aquifer releases from storage water per surface area unit of aquifer per unit decline in the GWD" (Freeze, Cherry, 1979). The contribution was calculated as a percent of ET_a based on the equivalent depth of water released by the GWD drop. However, these differences represented approximately the contribution of GW to crop ET in the daytime (ET_D) which represents the majority (about 90%) of full-day ET (ET_{24}) according Gribovszki et al. (2010) as follows:

$$ET_{gw} = GWDdrop * specificsoilyield * 1.1 (for 24hr) \tag{6}$$

The spatial variability of GWD for different parts within the study area was done using Ordinary Kriging, according to (Eberly et al., 2004).

3. Results

3.1. Crop water requirements

The estimated ET_{LS} rate in the study area followed a typical seasonal pattern with a gradual rise in daily ET_{LS} rates from May to August due to the peak of the growing season and crop water requirements. This increase is a result of air temperature in the summer being much higher, while there was a steady decrease in ET_{LS} from September to February. The low frequency of precipitation from mid-November to February created a lower daily ET_{LS} rate. The results obtained from the satellite images indicated that the mean daily ET_{LS} decreased significantly from 6.4 mm day^{-1} in July of 2017–1.6 mm day^{-1} in January of 2018. This was followed by a gradual increase, from February to May, with ET_{LS} of 5.7 mm day^{-1} for June 2018 (Table 2 and Fig. 3). The mean value of ET_{LS} was 5.9 mm day^{-1} in the summer season, 3.6 mm day^{-1} in the autumn season, and 2.7 mm day^{-1} in the winter season, while it was

Table 1
Satellite images (Path 177 and Row 38), acquisition date, and day of the year (DOY) for the study area.

Acquisition date	DOY	Acquisition ate	DOY
July,4, 2017	185	January,12, 2018	12
August, 5, 2017	217	February,13, 2018	44
September,6, 2017	249	Mach,17, 2018	75
October,8, 2017	281	April, 18, 2018	108
November,9, 2017	313	May,20, 2018	140
December,11, 2017	345	June, 21,2018	172

4.8 mm day^{-1} in the spring season.

The statistical analysis indicated that the crop evapotranspiration (ET_a) estimated using the climate data (ET_{ec}) values for different months are close to those estimated using Landsat Satellite (ET_{LS}) with a coefficient of determination (R^2) value of 0.89, as shown in Eq. 3 and Eq. 9. For different parts of the study area, the values of ET_{ec} are correlated to ET_{LS} values, according to R^2 (0.84–0.90), as shown in Table 3 and Fig. 3.

< mmEquation id = "eqn1"/ > (7)

3.2. Effect of groundwater depth

The GWD values varied during the study period according to the location, the planted crops, and the estimation time (a month or the time from irrigation events). The GWD in different parts of the study area ranged from 72.9 to 138.2 cm below the soil surface, with a mean value of 107.4 cm (Table 4). The ET_{LS} values were mainly affected by climatic conditions over the study area, but its values in different parts were moderately affected by GWD ($R^2 = 0.55$), as shown in Figs. 4–6.

Also, there was a correlation between ET_{LS} and GWD. ET_{LS} value decreased from 4.3 to about 4.0 mm day^{-1} when GWD increased from 75 cm to about 120 cm, but it increased again to about 4.4 mm day^{-1} with an increase in the GWD to about 140 cm. Therefore, the highest ET_{LS} value of 4.46 mm day^{-1} was achieved in part 1 with the deepest groundwater (138.2 cm), followed by ET_{LS} of 4.31 mm day^{-1} in part 3 with the shallowest groundwater (72.9 cm). On the other hand, the lowest ET_a values (4.08, 4.09, and 4.15 mm day^{-1}) were recorded in parts 6, 2, and 5 with GWD of 135.5, 110.5, and 95.3 cm, respectively. The healthy vegetation cover may also impact ET_{LS} value in addition to GWD. Therefore, the highest ET_{LS} value was recorded in part 1 with the deepest GW and good aeration condition in the effective root zone, which led to better vegetation cover. In part 3, shallow GW encourages the ET process, while the relatively high soil salinity level (7.47 dS m^{-1}) restricts this process, so a moderate ET_{LS} value was recorded.

3.3. Effect of soil salinity

The variation in soil salinity (EC_e) in the root zone of different parts of the area is relatively small since its mean values ranged from 4.6 to 7.5 dS m^{-1}, as shown in Table 3. It can be observed that ET_{LS} is slightly affected by (EC_e), while it is negatively and significantly affected by GWD as shown in the following polynomial equation:

$$ET_{LS} = 15.3 - 0.1476 * (GWD) + 0.0005 * (EC_e)^2 \; (R^2 = 0.87) \tag{8}$$

The effect of soil salinity, GWD, and the health of the vegetation cover on ET_{LS} cannot be separated easily. Therefore, the lowest ET_{LS} value, 4.08 mm day$^{-1,}$ was recorded in part 2 with EC_e of 5.68 dS m^{-1} and moderate GWD (110.5 cm), while the highest ET_{LS} value of 4.37 mm day^{-1} was achieved in part 1 with an EC_e value of 4.61 dS m^{-1} and the deepest GW (138.2 cm).

3.4. Contribution of groundwater

ET_{gw} is difficult to measure directly, but it could be predicted using the diurnal cycle of GWD caused by ET processes. The GWD varied according to the time of estimation, daylight, or nighttime. Thus, the ET_{gw} value can be calculated based on the diurnal cycle of GWD during the study period. According to Gribovszki et al. (2010), the water consumption of vegetation is the most important factor affecting the diurnal fluctuation of GW in temperate climates. This method assumes that the GW inflow rate is constant for the entire day (Loheide et al., 2005). However, the diurnal fluctuations of GW are due to crop water uptake because the lateral GW flux in day and night are omitted by subtracting the night GW value from its value in the daytime. Therefore, the effect of lateral GW flux on GW contribution to ET_{LS} is avoided. In a typical diurnal cycle in well-drained soils, the GWD declines rapidly during daylight due to ET by plants that extract the moisture from the root zone and utilize a portion of GW, leading to deeper GW. In this case, GWD rebounds again during night hours due to quick lateral and vertical GW flows (Loheide et al., 2009). In the case of the converse diurnal cycle in poorly drained soils, as observed in parts 3, 4, and 5 (Table 4), the low rate of GW flux cannot replenish this utilized moisture completely in the day-time, and therefore, GWD is not affected significantly during the day-time. In this condition, the utilized moisture during daytime

Table 2
Values of ET_{LS} (mm day^{-1}) for each part[a] in the different months.

Part	2017						2018						
	July	Aug.	Sept.	Oct.	Nov.	Dec.	Jan.	Feb.	March	April	May	June	Mean
P 1	6.60	6.00	5.50	4.40	3.40	3.00	1.60	2.80	3.50	4.10	6.20	6.40	4.46
P 2	6.20	5.60	4.90	4.10	3.40	3.00	1.50	2.80	3.40	3.50	5.10	5.60	4.09
P 3	6.80	6.60	5.10	4.20	3.40	2.90	1.60	3.00	3.70	3.80	4.80	5.80	4.31
P 4	6.20	6.50	5.20	4.30	3.30	3.00	1.50	2.80	3.50	3.80	4.90	5.50	4.21
P 5	6.20	5.50	5.10	4.20	3.40	3.00	1.70	2.80	3.60	3.80	4.90	5.60	4.15
P 6	6.20	5.80	5.30	4.40	3.40	3.00	1.40	2.90	3.50	3.50	4.30	5.30	4.08
Mean ET_{LS}	6.37	6.00	5.18	4.27	3.38	2.98	1.55	2.85	3.53	3.75	5.03	5.70	4.22
Mean ET_{ec}	8.53	7.43	5.31	4.60	1.84	1.77	1.56	2.55	2.73	3.12	5.50	8.07	4.40

[a] Statistical comparison between ET_{LS} and ET_{ec} for different months: $R^2 = 0.89$ the area was divided into six parts, as shown in Fig. 1.

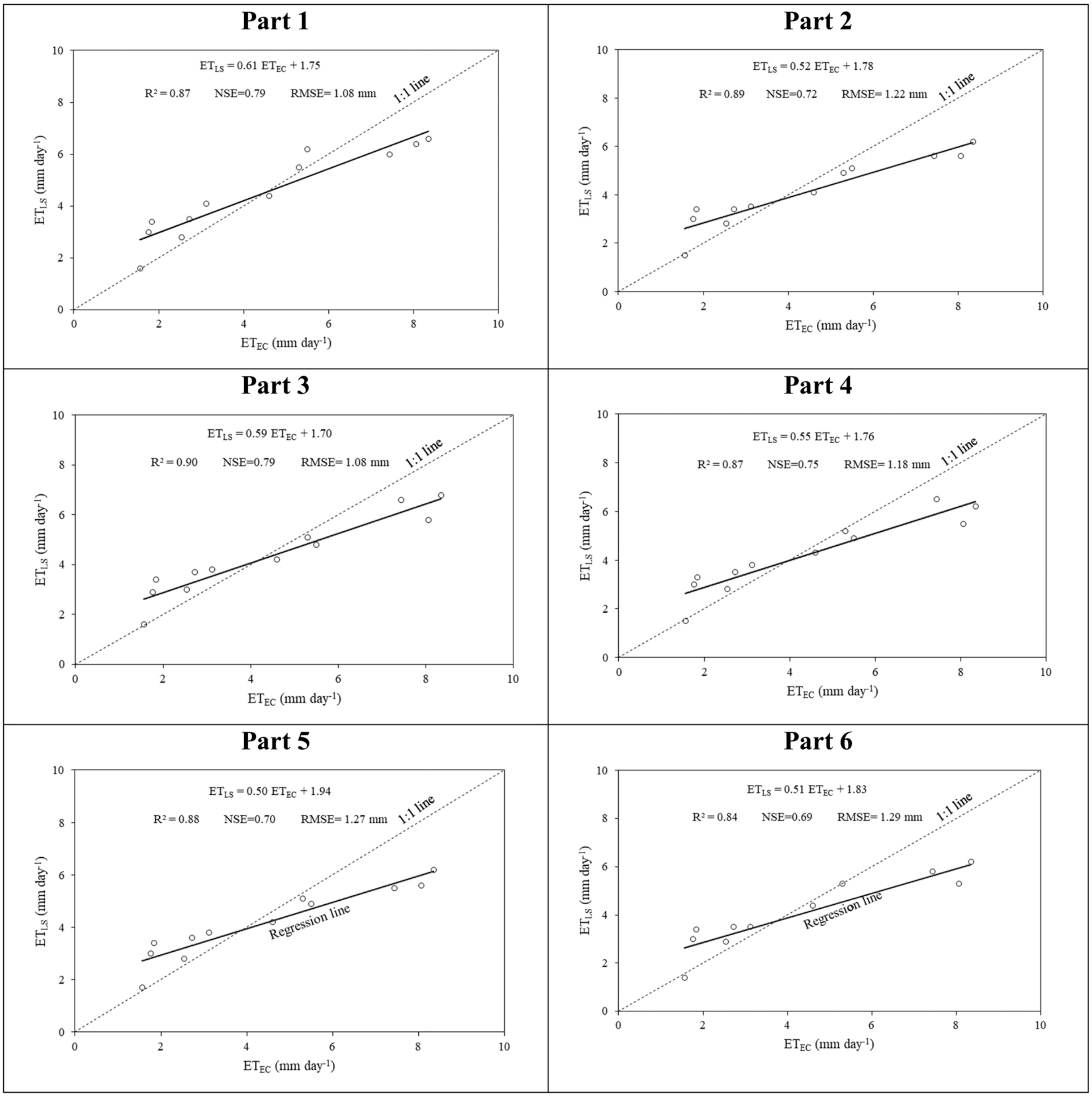

Fig. 3. Comparison between ET_{LS} and ET_{ec} values (mm day^{-1}) for each part.

Table 3
Statistical comparison between ET_{LS} and ET_{ec} values (mm day^{-1}) for each field part.

Location	Mean							Regression	
	ET_{ec}	ETLS	RMSE	RMSE%	MBE	MBE%	NSE	R^2	Slope
Part 1	4.40	4.46	1.08	24.56	-0.06	-1.26	0.79	0.87	0.61
Part 2	4.40	4.09	1.22	27.93	0.31	7.06	0.72	0.89	0.52
Part 3	4.40	4.31	1.08	24.70	0.09	2.14	0.79	0.90	0.59
Part 4	4.40	4.21	0.19	26.96	0.19	4.41	0.75	0.87	0.55
Part 5	4.40	4.15	1.27	28.99	0.25	5.73	0.70	0.88	0.50
Part 6	4.40	4.08	1.29	29.38	0.32	7.24	0.69	0.84	0.51

Table 4
Relationship between ET_{LS} and both GWD and EC_e.

Location	GWD (cm)	EC_e (dS m^{-1})	ET_{LS} (mm day^{-1})
Part 1	-138.2	4.61	4.46
Part 2	-110.5	5.68	4.09
Part 3	-72.9	7.47	4.31
Part 4	-91.8	5.93	4.21
Part 5	-95.3	5.27	4.15
Part 6	-135.5	4.64	4.08
Mean	-107.4	5.62	4.22

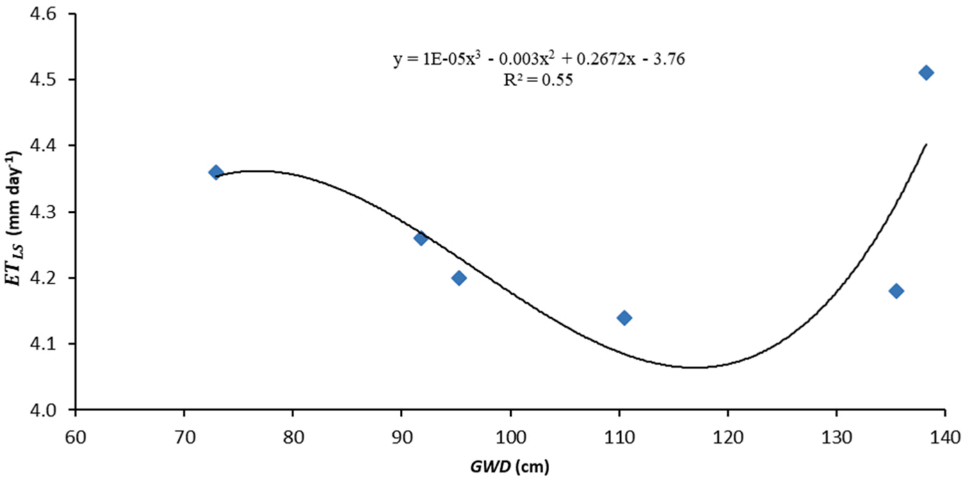

Fig. 4. Relationship between ET_{LS} (mm day^{-1}) and GWD (cm).

is completely replenished by GW flux, leading to deeper GW in the night (Cordeiro et al., 2015), as shown in Table 5 and Supplementary Figure 2. Moreover, Table 2 shows that the variations of ET_{gw} values in the various months are related to the climate conditions, GWD, and planted crops, deep or shallow-rooted, which influence the GWD and ET. Therefore, the highest ET_{gw} values ranged from 1.32 to 1.72 mm day^{-1} during June, July, October, and November, where the GWD was in the range of 60–75 cm. The lowest ET_{gw} values ranged from 0.79 to 1.06 mm day^{-1} from December to May, with a GWD range of 75–100 cm. This means that the ET_{gw} value depended on GWD with a strong negative correlation (R^2 = 0.82) as shown in Fig. 7 with a GWD range of 75–100 cm or a very weak negative correlation (R^2 = 0.32) as shown in Fig. 8 with a GWD range of 75–100 cm. Hence, it could be observed from the statistical relationship that the ET_{gw} value was higher with shallower GWD (>75 cm) and then decreased with deeper GWD to 100 cm.

Concerning the effect of GWD in different parts of the area under study on $ET_{gw,}$ Table 6 shows that parts 2 and 5, with a GWD range of 102–111 cm, recorded the highest ET_{gw} values (42.1% and 44.9%, respectively). The lowest ET_{gw} value (22.4%) was recorded in part 6 with a GWD of 136 cm. There is a weak statistical correlation between ET_{gw} and GWD with different parts (R^2 = 0.32), as shown in Fig. 8 and Table 7, which indicated that ET_{gw} depends, in addition to GWD, on other factors, i.e., the planted crops and soil hydraulic conductivity.

Regardless of the effect of time or location of measurements, the ET_{gw} value was somewhat affected by the planted crops. Table 7 and S.Fig. 3 indicate that summer crops achieved ET_{gw} values higher than winter crops (1.7 and 1.2 mm day^{-1}, respectively). The GW covered about 1.6 and 1.7 mm day^{-1} (32.0% and 34.0%) of water requirements of seed melon and cotton, respectively, while it contributed about 0.9 mm day^{-1} (22.5%) for sugar beet and 1.3 mm day^{-1} for clover (28.9%) and wheat (37.1%).

4. Discussion

4.1. Factors affecting evapotranspiration

Many factors are affecting ET in arid regions, including but not limited to deficit irrigation and limited water resources (Ding, and Kheir et al., 2021, 2021) as well as climate change (Ali et al., 2020). However, additional factors of salinity and groundwater and their relationship with ET has received less attention so far, proving the significance of the current investigation. The ET_{LS} rate in this study followed a normal seasonal pattern with a gradual rise in daily ET_{LS} rates through the summer growing season and a steady decrease in ET_{LS} through the winter growing season. The ET_{LS} values were compared versus the ET_{ec} values calculated directly from the data to assess their validity. Therefore, coefficient of determination (R^2), simple correlation coefficient (r), and t-test were used. The statistical analysis indicated that the ET_{LS} values are close to those estimated from the climate data through the values of R^2 (0.87), r (0.86), and

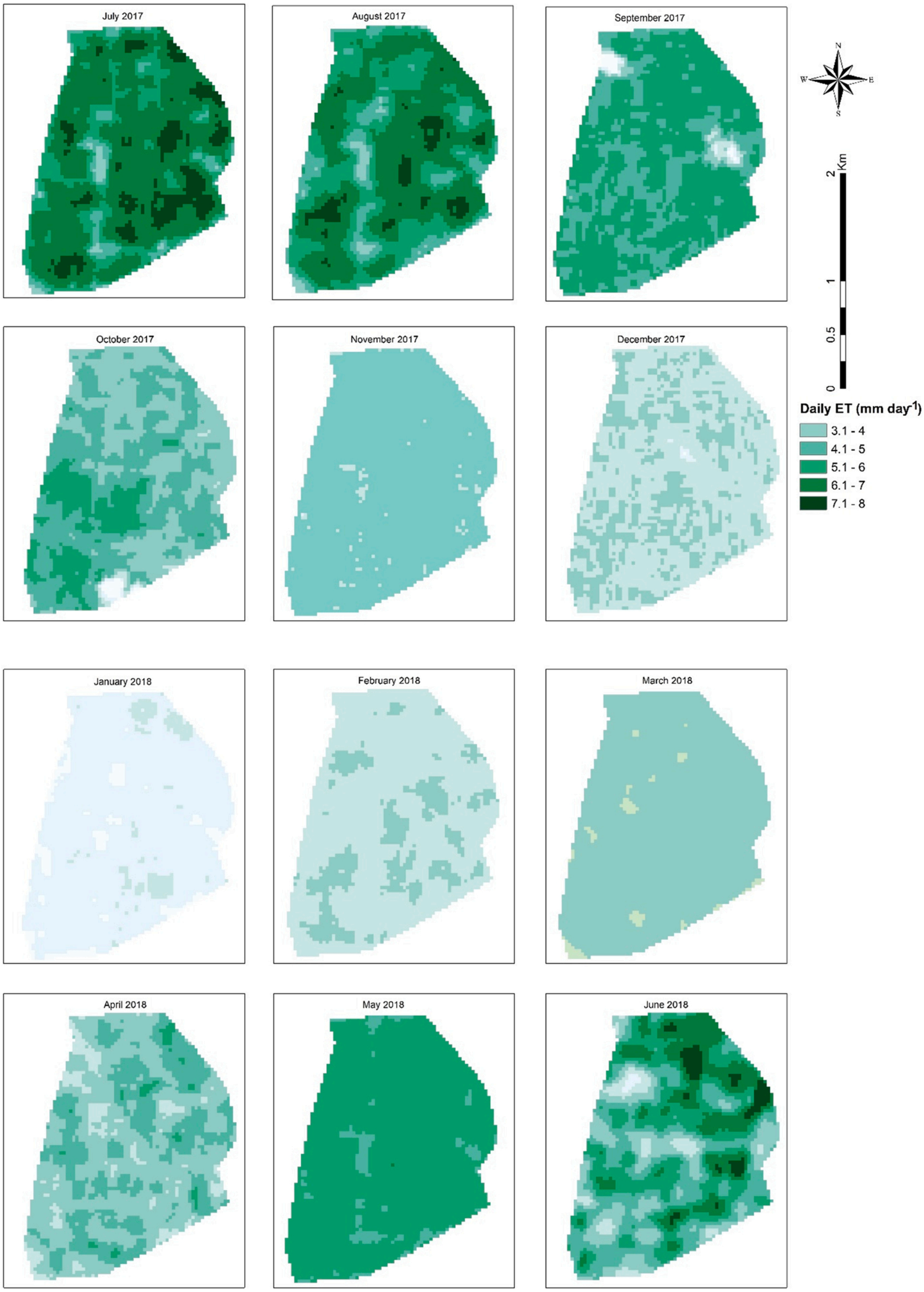

Fig. 5. ET_{LS} for different months for 2017 and 2018 obtained from the LANDSAT 8 Satellite Images.

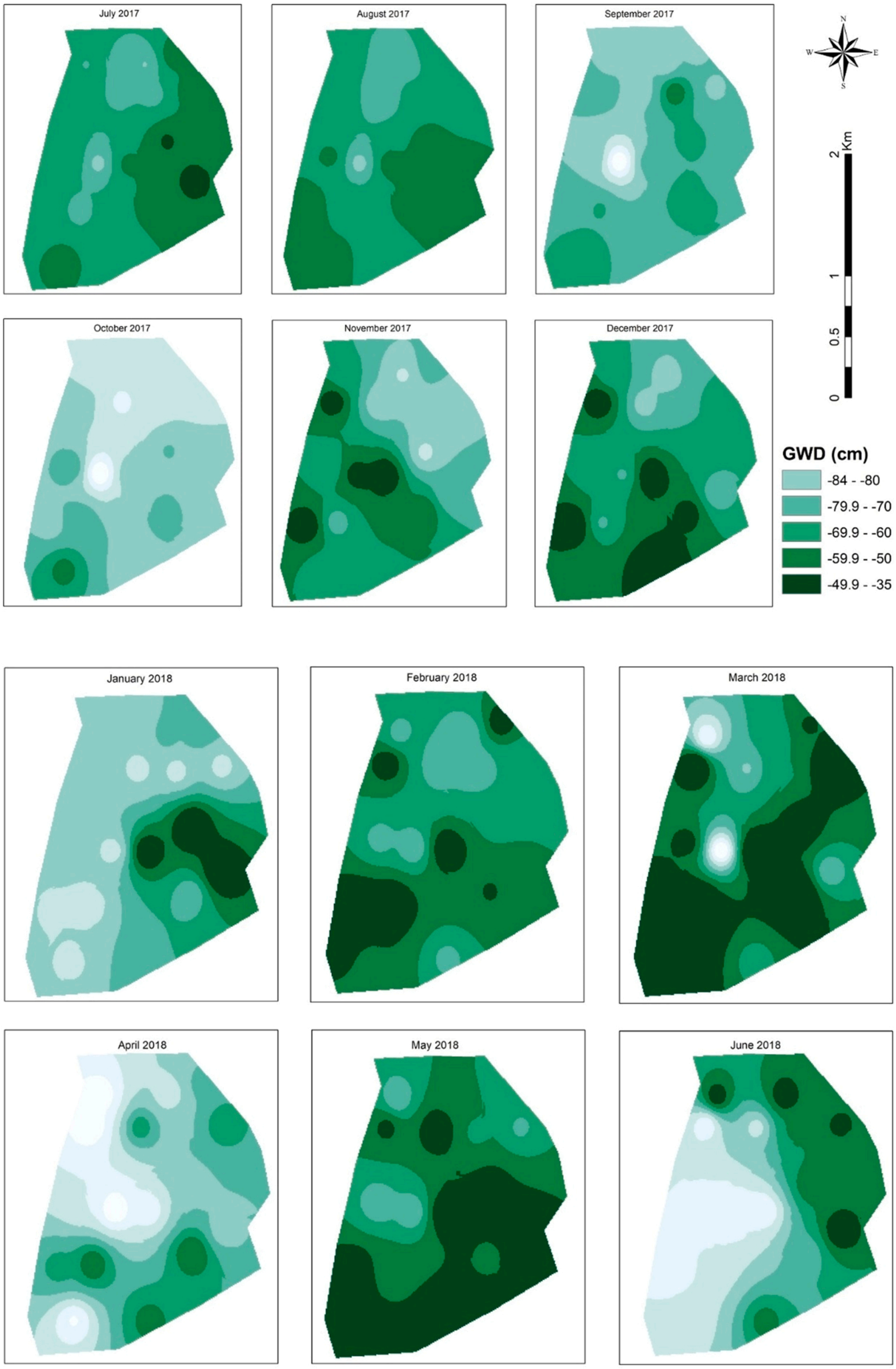

Fig. 6. GWD in different parts for 2017 and 2018 obtained by the Kriging method.

p-value is highly significant, as shown in Tables 1 and 2. Also, the ET_{LS} values estimated in this study are similar to previous studies conducted in the same area (El-Mowelhi, and EL-Bialy et al., 1995, 2009). In addition, satellite-based ET is preferable in order to aggregate spatial heterogeneities that can bias interpretation from point measurements.

Table 5
Effect of GWD on ET_{gw} for different months.

Month	Daylight (cm)	Night (cm)	GWD drop (mm)	ET_{gw} (mm day-1)	ET_{gw} (%)
July	-77.0	-75.8	12.0	1.58	24.3
August	-75.8	-75.0	8.0	1.06	26.6
September	-88.1	-87.3	8.0	1.06	24.8
October	-94.7	-93.7	10.0	1.32	20.3
November	-69.1	-68.1	10.0	1.32	36
December	-90.3	-89.5	8.0	1.06	25
January	-66.9	-66.3	6.0	0.79	37
February	-77.2	-76.6	6.0	0.79	29.5
March	-90.2	-89.4	8.0	1.06	26.2
April	-99.6	-98.8	8.0	1.06	15.1
May	-95.2	-94.4	8.0	1.06	18.6
June	-72.0	-70.7	13.0	1.72	30.1
Mean	-83.0	-82.1	9.0	1.19	26.13
Summer	-82.5	-81.6	9.0	1.19	23.25
Winter	-83.5	-82.7	8.2	1.08	29

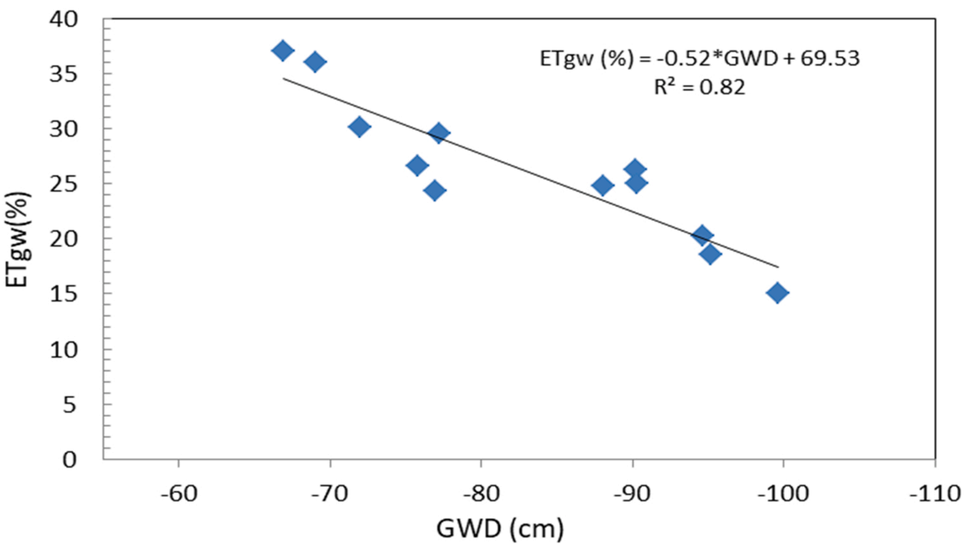

Fig. 7. Groundwater contribution to crop water use (ET_{gw} %) with a GWD in different months.

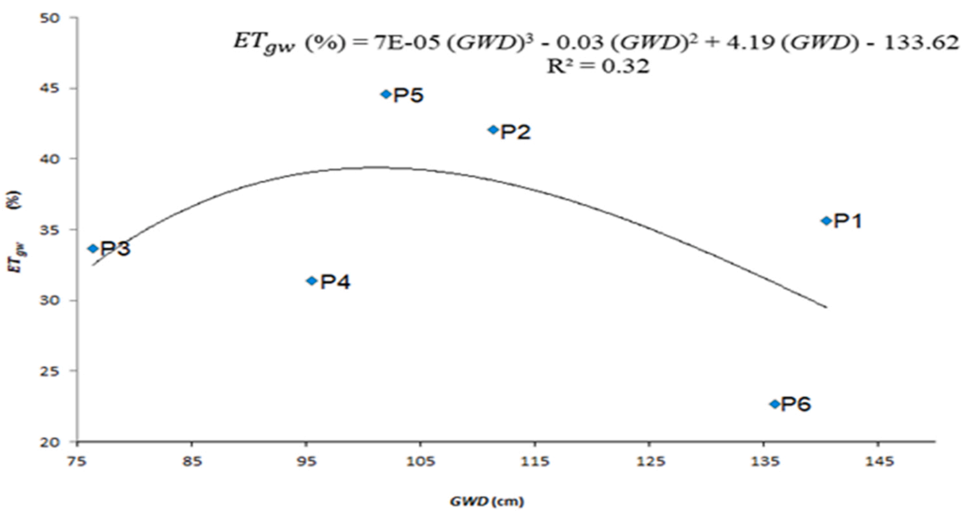

Fig. 8. Groundwater contribution to water use (ET_{gw} %) of the crops grown in different parts (P1, P2, P3, P4, P5, and P6) of the study area.

Table 6
Effect of GWD on ET_{gw} of plant cover.

Part	Daylight (cm)	Nighttime (cm)	GWD drop (mm)	ET_{gw} (mm day-1)	ET_{gw} (%)	Dropdown rate (cm day^{-1})	
						After 48 hr from irrigation	Entire-time between irrigations
Part $_1$	-140.5	-139.3	12.0	1.58	36.2	31.2	7.4
Part $_2$	-111.4	-110.1	13.0	1.72	42.1	22.8	3.2
Part $_3$	-76.4	-77.5	11.0	1.45	33.7	15.1	6.5
Part $_4$	-95.5	-96.5	10.0	1.32	31.1	14.6	5.3
Part $_5$	-102.0	-103.4	14.0	1.85	44.9	22.0	7.1
Part $_6$	-136.0	-135.3	7.0	0.92	22.4	26.9	5.9

Table 7
Contribution of GW to water use (ET_{gw}) with different crops.

Crop	Daylight (cm)	Nighttime (cm)	GWD drop (mm)	ET_{gw} (mm day^{-1})	ET_{gw} (%)
S. Beet	-78.5	-77.8	7.0	0.9	22.5
Wheat	-109.6	-108.6	10.0	1.3	37.1
Clover	-60.3	-59.3	10.0	1.3	28.9
Cotton	-113.2	-111.9	13.0	1.7	34.0
S. melon	-76.7	-77.9	12.0	1.6	32.0
Winter crops	-82.8	-81.9	9.0	1.2	30.0
Summer crops	-95.6	-94.3	12.5	1.7	34.0

4.2. *Effect of groundwater depth*

The GWD values in this study were affected by location and time of estimation (during the day or at night), and the planted crops (Table 5). The ET_{LS} values were mainly affected by climatic conditions in the area, but ET_{LS} values in various parts were moderately affected by GWD. Also, there was a variable trend between ET_{LS} and GWD; see Figs. 5–7. This non-linear trend may be due to the ET_{LS} value being affected by GWD in addition to factors such as soil, GW salinity, and irrigation frequency, as reported by (Karimov et al., 2014). The healthy vegetation cover may also impact ET_{LS} values in addition to GWD. This phenomenon is similar to that observed by (Prathapar and Qureshi, 1999b), who reported that shallow GW could contribute to ET_{LS} by up to 80% without affecting crop yield and soil salinization. Other studies also reported the variable response of ET_{LS} to GWD under certain conditions. For example, Lafleur and Roulet (1992) found a strong response of ET to GWD, and (Lafleur et al., 2005) found a moderate or threshold type response between them, but no significant effect of GWD on ET_{LS} was observed by (Wu et al., 2010). Also, Moore et al. (2013) reported an insignificant relationship between ET and GWD in peatlands.

4.3. *Effect of soil salinity*

The variations in ET_{LS} values for different study parts are relatively small, and their values are slightly higher than those estimated by the ET_{ec} method. It can be observed that ET_{LS} is slightly affected by ET_a, while it is negatively and significantly affected by GWD, as shown in equation (7). Also, the effect of soil salinity, GWD, and the health of the vegetation cover on ET_{LS} cannot be separated easily. Therefore, the low value of ET_{LS} in some locations in the study area may be due to increased water potential in the surface layer and decreased biomass yield due to increases in the energy expended by the plant to extract water from the root zone soil. Other studies used the Surface Energy Balance System (SEBS) to estimate atmospheric turbulent fluxes and evaporative fractions by combining satellite earth observation data with meteorological information at appropriate scales with acceptable accuracy(Su, 2002). In comparison to this study, our approach linked ET_{EC} observations with Landsat images ET_{LS} to achieve robust results. These findings agree with those obtained by (Cemek et al., 2011), who reported that the relationships between ET, soil salinity, and yield were generally linear with increasing or decreasing tendencies. Also, Ünlükara et al. (2008) observed a decrease in water consumption of okra due to soil salinity with a threshold value of 3.48 (dS m^{-1}).

4.4. *Contribution of groundwater*

ET_{gw} could be predicted by the diurnal cycle of GWD caused by ET processes. The GWD varied according to the time of estimation, daylight, or nighttime. In normal soil, the diurnal fluctuations in water levels reflect the uptake of GW by plants, where the drawdown of water levels occurs during daylight hours (Loheide et al., 2009). However, the converse diurnal cycle observed in some parts may be due to poorly drained soils expressed as a low dropdown rate of groundwater level, as shown in Table 7. Therefore, the soil became drier during high ET demand in the daylight and became wetter during low ET in the evening and night (Cordeiro et al., 2015). Consequently, GW became deeper during the night, as shown in Fig. 8.

ET_{gw} values affected by the climate conditions, GWD, and the planted crops, deep or shallow-rooted, influence the GWD and ET. The ET_{gw} value depended significantly on GWD with a negative correlation, as shown in Fig. (8). The observation of (Chen and Hu,

2004) and (Chimner and Cooper, 2004) confirms these results, who reported that GWD within 2 m of the soil surface might have sufficient capillary rise to supply water to plants. Shah et al. (2007b) recognized the contribution from shallow GW to plant evaporative demand. As a result, the decrease in ET rates may be caused by lowering the GWD concerning plant roots. Additionally, Ayars et al. (2006) observed that the GW near the bottom of the root zone might act as a valuable water source through the capillary rise, which supplies the plant with 50% of the total ET according to its depth.

Also, a weak statistical correlation between ET_{gw} and GWD for different parts (Fig. 8) indicated that ET_{gw} depends, in addition to GWD, on other conflicting factors, i.e., the planted crops and soil hydraulic conductivity. The ET_{gw} value was somewhat affected by the planted crops. Summer crops achieved ET_{gw} values higher than those of winter crops. The relatively low value of ET_{gw} with winter crops may be due to the rain events, which replenish a significant part of soil moisture and can be absorbed by plant roots. Also, most winter crops are relatively shallow-rooted, and in addition, the evaporation rate in the winter season is relatively low. Thus, the values of ET_{gw} with the investigated summer crops were relatively high, which may be attributed to 1) cotton is deep-rooted and therefore has greater ability to withdraw shallow GW, and 2) seed melon needs to withdraw part of GW because its irrigation interval is relatively long and it has a dense root system. (Shah et al., 2007a) confirmed that the connecting of GW and root zone depends on the soil texture and begins at GWD between 30 and 100 cm for deep-rooted vegetation.

Also, remote sensing estimates of ET_{LS} and the contribution of GW to ET_{LS} are continuously and widely used due to understanding the relationship between the ET spatial variability and groundwater level. They are easy to use and save time and costs, especially with open access databases, although they may be less accurate than direct measurements. However, remote sensing-based methods have some limitations because most parameters cannot be directly observed but must be calculated indirectly from satellite observations via retrieval algorithms. Furthermore, satellite retrievals are bound to contain errors, which will eventually bias the application of remote sensing, necessitating their coupling with actual observations to be validated and improved.

5. Conclusions

ET_{LS} values in the study area were moderately affected by GWD. The ET_{LS} values were decreased when GWD increased up to 120 cm, but its values increased with increasing GWD up to 140 cm. Evapotranspiration was significantly affected by soil salinity and groundwater depth (R^2 =0.87). ET_{gw} values in different months depended mainly on GWD with a negative correlation ($R^2 = 0.61$), and about 1.2 mm day^{-1} of the crop water use was supplied from shallow GW (<90 cm). Statistical analysis demonstrated that shallow GW contributed significantly to various crops' water use with noticeable differences in rates. The summer crops achieved higher values of ET_{gw} than those of winter crops by 29.4%, the GW contributed 1.7 and 1.6 mm day^{-1} of cotton and seed melon crop water requirements, respectively, while it contributed 0.9 mm day^{-1} for sugar beet and 1.3 mm day^{-1} for both wheat and clover. The study also showed that remote sensing and GIS techniques are valuable tools for evaluating the influence of shallow GW and soil salinity on ET_{LS} and ET_{gw} in large geographic areas with relatively low costs. Also, both remote sensing estimates of ET_{LS} and the contribution of GW to ET_{LS} are widely used due to their applicability and relationship representation between ET spatial variability and groundwater level, even though these techniques may be less accurate than direct measurements. Further, the statistical analysis indicated that the ET_{LS} values are correlated to those estimated directly from climate data.

CRediT authorship contribution statement

Hesham M. Aboelsoud: Conceptualization, Methodology, Software. **Ayman Habib:** Data curation, Writing – original draft preparation, Project administration. **Bernard Engel:** Data curation, Writing – original draft preparation, Supervision. **Ahmed A. Hashem:** Visualization, Investigation. **Waleed Abou El-Hassan***:* Resources. **Ajit Govind:** Data curation, Writing – original draft preparation. **Ahmed Kheir**: Conceptualization, Software, Formal analysis, Writing – original draft, Writing – review & editing. **Abdelrazek Elnashar:** Software, Validation. **Mona Eid:** Methodology, Investigation, Writing – review & editing

Declaration of Competing Interest

The authors declare that they have no known competing financial interests or personal relationships that could have appeared to influence the work reported in this paper.

Data Availability

Data will be made available on request.

Acknowledgments

The authors acknowledge the Soils, Water and Environment Research Institute (SWERI), Agric. Res. Centre (ARC), Egypt and the Agricultural & Biological Engineering Department, Purdue University, the USA, for their scientific, technical, and financial support. The authors also acknowledge the ICARA Project N. LWR/2011/045 titled "Management of Water and Salinity in the Nile Delta" for providing sensors used to record the ground-water depths. We also acknowledge the CGIAR Excellence in Agronomy-Egypt Use Case (https://www.cgiar.org/initiative/11-excellence-in-agronomy-eia-solutions-for-agricultural-transformatio).

Appendix A. Supporting information

Supplementary data associated with this article can be found in the online version at doi:10.1016/j.ejrh.2023.101372.

References

Aboelnour, M., Engel, B.A., 2018. Application of remote sensing techniques and geographic information systems to analyze land surface temperature in response to land use/land cover change in Greater Cairo Region, Egypt. J. Geogr. Inf. Syst. 10 (01), 57–88.

Aboelsoud, H.M., Abdelrahman, M.A.E., 2017. Rapid field technique for soil salinity appraisal in North Nile Delta Using EM 38 through some empirical relations. Int. J. Plant Soil Sci. 14 (5), 1–9.

Ali, M.G.M., Ibrahim, M.M., El Baroudy, A., Fullen, M., Omar, E.-S.H., Ding, Z., Kheir, A.M.S., 2020. Climate change impact and adaptation on wheat yield, water use and water use efficiency at North Nile Delta. Front. Earth Sci. 522–536.

Arasteh, P.D., Tajrishy, M., 2008. Calibrating Priestley-Taylor model to estimate open water evaporation under regional advection using volume balance method-case study: Chahnimeh reservoir, Iran. J. Appl. Sci. 8 (22), 4097–4104.

Aubinet, M., Vesala, T., Papale, D., 2012. Eddy Covariance: A Practical Guide to Measurement and Data Analysis. Springer Science & Business Media.

Ayars, J.E., Christen, E.W., Soppe, R.W., Meyer, W.S., 2006. The resource potential of in-situ shallow ground water use in irrigated agriculture: a review. Irrig. Sci. 24 (3), 147–160.

Ayars, J.E., Shouse, P., Lesch, S.M., 2009. In situ use of groundwater by alfalfa. Agric. Water Manag. 96 (11), 1579–1586.

Baldocchi, D., 2014. Measuring fluxes of trace gases and energy between ecosystems and the atmosphere–the state and future of the eddy covariance method. *Glob. Change Biol.* 20 (12), 3600–3609.

Black, C.A., 1965. *Methods of Soil Analysis*. *American Society of Agriculture*, Madison, Wisconsin.

Campbell, J.B., 1996. Introduction to remote second edition, second ed. The Guilford Press, *London*.

Cemek, B., Ünlükara, A., Karaman, S., Gökalp, Z., 2011. Effects of evapotranspiration and soil salinity on some growth parameters and yield of lettuce (Lactuca sativa var. crispa). *Agriculture* 98 (2), 139–148.

Chen, X., Hu, Q., 2004. Groundwater influences on soil moisture and surface evaporation. J. Hydrol. 297 (1–4), 285–300.

Chimner, R.A., Cooper, D.J., 2004. Using stable oxygen isotopes to quantify the water source used for transpiration by native shrubs in the San Luis Valley, Colorado U.S.A. Plant Soil 260 (1–2), 225–236.

Cooper, D.J., Sanderson, J.S., Stannard, D.I., Groeneveld, D.P., 2006. Effects of long-term water table drawdown on evapotranspiration and vegetation in an arid region phreatophyte community. J. Hydrol. 325 (1–4), 21–34.

Cordeiro, M.R.C., Krahn, V., Ranjan, R.S., Sager, S., 2015. Water table contribution and diurnal water redistribution within the corn root zone. Can. Biosyst. Eng. / Le. Genie Des. Biosyst. au Can. 57 (1), 139–148.

Devitt, D.A., Donovan, D.J., Katzer, T., Johnson, M., 2002. A reevaluation of the ground water budget for Las Vegas Valley, Nevada, with emphasis on ground water discharge. J. Am. Water Resour. Assoc. 38 (6), 1735–1751.

Dinar, A., Rhoades, J.P., Nash, P., Waggoner, B.L., 1991. Production functions relating crop yield, water quality and quantity, soil salinity and drainage volume. Agric. Water Manag. 19 (1), 90062.

Ding, Z., et al., 2020a. The integrated effect of salinity, organic amendments, phosphorus fertilizers, and deficit irrigation on soil properties, phosphorus fractionation and wheat productivity. Sci. Rep. 10 (1), 2736.

Ding, Z., Koriem, M.A., Ibrahim, S.M., Antar, A.S., Ewis, M.A., He, Z., Kheir, A.M.S., 2020b. Seawater intrusion impacts on groundwater and soil quality in the northern part of the Nile Delta, Egypt. Environ. Earth Sci. 1–11.

Ding, Z., Ali, E.F., Elmahdy, A.M., Ragab, K.E., Seleiman, M.F., Kheir, A.M.S., 2021. Modeling the combined impacts of deficit irrigation, rising temperature and compost application on wheat yield and water productivity. Agric. Water Manag., 106626

Eberly, S., Swall, J., Holland, D., Cox, B., Baldridge, E., 2004. Developing spatially interpolated surfaces and estimating uncertainty. Quality 169.

EL-Bialy, M.A. A. (2009). "Irrigation water management of rice crop. Ph.D., Thesis, Fac. of Agric., Mansoura Univ. Egypt.

El-Ghannam, M., Abdel-Razek, M.K., and Abo El-Soud, H. (2019). "Quality assessment of some water sources and soil under sea water intrusion conditions in north Nile Delta, Egypt." Environment, Biodiversity and Soil Security, The National Centre for Information and Documentation (NIDOC), the Academy …, 3(2019), 179–192.

Elhaddad, A., Garcia, L.A., Gates, T.K., 2007. A remote sensing - GIS approach to evaluate the effects of soil salinity on evapotranspiration. Hydrol. Days 2007 2 (970), 80523.

El-Kiki, M.H. (2018). "Effect of sea water intrusion on Nile Delta and possible suggested solution."

El-Mowelhi, N.M., Abo Soliman, M.S.M., Shams El-Din, H.A., Ayars, J., and Hasanein, S.A. (1995). "On farm water management in soils of Kafr El-Sheikh. II. Evaluation of land leveling practices and stream size under furrow irrigation system." Soil and Water Res. Int., Agric. Res. Center., Conf. on Farm irrigation and Agroclimatology 2–4 January, Dokki Egypt, 157–164.

Freeze, R.A., Cherry, J.A. (1979). Groundwater. (Cathy Brenn and K. McNeily, eds.), Prentice-Hall, Inc. Englewood Cliffs, New Jersey 07632, New Jersey United States of America.

Fujimaki, H., Shimano, T., Inoue, M., Nakane, K., 2006. Effect of a salt crust on evaporation from a bare saline soil. Vadose Zone J. 5 (4), 1246–1256.

Gan, G., et al., 2020. Seasonal and diurnal variations in the Priestley–Taylor coefficient for a large ephemeral lake. Water 12 (3), 849.

Gribovszki, Z., Szilágyi, J., Kalicz, P., 2010. Diurnal fluctuations in shallow groundwater levels and streamflow rates and their interpretation - a review. *J. Hydrol.* 385 (1–4), 371–383.

Hu, G., Jia, L., Menenti, M., 2015. Comparison of MOD16 and LSA-SAF MSG evapotranspiration products over Europe for 2011. Remote Sens. Environ. 510–526.

Huo, Z., Feng, S., Huang, G., Zheng, Y., Wang, Y., Guo, P., 2012. Effect of groundwater level depth and irrigation amount on water fluxes at the groundwater table and water use of wheat. Irrig. Drain. 61 (3), 348–356.

Iritz, Z., Lindroth, A., 1994. Night-time evaporation from a short-rotation willow stand. J. Hydrol. 157 (1–4), 235–245.

Jackson, M.L. (1967). Soil Chemical Analysis - Advanced Course. Public. By the author, Dept. of Soils, Univ. of Wise. Madison 6, Wishensin, USA.

Jat, R.D., Jat, H.S., Nanwal, R.K., Yadav, A.K., Bana, A., Choudhary, K.M., Kakraliya, S.K., Sutaliya, J.M., Sapkota, T.B., Jat, M.L., 2018. Conservation agriculture and precision nutrient management practices in maize-wheat system: effects on crop and water productivity and economic profitability. Field Crop. Res. 111–120.

Jiang, L., Islam, S., 1999. A methodology for estimation of surface evapotranspiration over large areas using remote sensing observations. Geophys. Res. Lett. 26 (17), 2773–2776.

Kahlown, M.A., Ashraf, M., Haq, Z., 2005. Effect of shallow groundwater table on crop water requirements and crop yields. Agric. Water Manag. 76 (1), 24–35.

Kang, S., Zhang, F., Hu, X., Jerie, P., Zhang, L., 2001. Effects of shallow water table on capillary contribution, evapotranspiration, and crop coefficient of maize and winter wheat in a semi-arid region. Aust. J. Agric. Res. 52, 317–327.

Karimov, A.K., Šimůnek, J., Hanjra, M.A., Avliyakulov, M., Forkutsa, I., 2014. Effects of the shallow water table on water use of winter wheat and ecosystem health: Implications for unlocking the potential of groundwater in the Fergana Valley (Central Asia). Agric. Water Manag. 131, 57–69.

Khatib, A.B., 1971. Present and potential salt-affected and waterlogged areas in the countries of the Near- East in relation to agriculture. Irrig. Drain. 7, 14–28.

Kheir, A.M.S., Alrajhi, A.A., Ghoneim, A.M., Ali, E.F., Magrashi, A., Zoghdan, M.G., Abdelkhalik, S.A.M., Fahmy, A.E., Elnashar, A., 2021. Modeling deficit irrigation-based evapotranspiration optimizes wheat yield and water productivity in arid regions. Agric. Water Manag., 107122

Kim, H.W., Hwang, K., Mu, Q., Lee, S.O., Choi, M., 2012. Validation of MODIS 16 global terrestrial evapotranspiration products in various climates and land cover types in Asia. KSCE J. Civ. Eng. 229–238.
Kurtzman, D., Scanlon, B.R., 2011. Groundwater recharge through vertisols: irrigated cropland vs. natural land, Israel. Vadose Zone J. 10 (2), 662–674.
Lafleur, P.M., Roulet, N.T., 1992. A comparison of evaporation rates from two fens of the Hudson Bay Lowland. Aquat. Bot. 44 (1), 59–69.
Lafleur, P.M., Hember, R.A., Admiral, S.W., Roulet, N.T., 2005. Annual and seasonal variability in evapotranspiration and water table at a shrub-covered bog in southern Ontario, Canada. Hydrol. Process. 19 (18), 3533–3550.
Li, S., Wang, G., Sun, S., Chen, H., Bai, P., Zhou, S., Huang, Y., Wang, J., Deng, P., 2018. Assessment of multi-source evapotranspiration products over china using eddy covariance observations. *Remote Sens.* 10 (11), 1692.
Lijuan, W., Ni, G., Sha, S., Die, H., Wei, W., 2016. The triangular method for evapotranspiration estimation from landsat data in arid and semi-arid regions. Int. Geosci. Remote Sens. 230–233.
Liu, T., Luo, Y., 2011. Effects of shallow water tables on the water use and yield of winter wheat ('Triticum aestivum'l.) Under rain-fed condition. Aust. J. Crop Sci. 5 (13), 1692.
Logsdon, S.D., Ramirez, Hernandez, G., Hatfield, J.L., Sauer, T.J., Prueger, J.H., 2009. Soil water and shallow groundwater relations in an agricultural hillslope. Soil Sci. Soc. Am. J. 73 (5), 1461.
Loheide, S.P., Butler, J.J., Gorelick, S.M., 2005. Estimation of groundwater consumption by phreatophytes using diurnal water table fluctuations: a saturated-unsaturated flow assessment. Water Resour. Res. 41 (7), 1–14.
Loheide, S.P., Deitchman, R.S., Cooper, D.J., Wolf, E.C., Hammersmark, C.T., Lundquist, J.D., 2009. A framework for understanding the hydroecology of impacted wet meadows in the Sierra Nevada and Cascade Ranges, California, USA. Hydrogeol. J. 17 (1), 229–246.
Mabrouk, M., Jonoski, A., Oude Essink, G.H.P., Uhlenbrook, S., 2019. Assessing the fresh–saline groundwater distribution in the Nile Delta aquifer using a 3D variable-density groundwater flow model. *Water*, Multidiscip. 11 (9), 1946.
Majozi, N.P., Mannaerts, C.M., Ramoelo, A., Mathieu, R., Mudau, A.E., Verhoef, W., 2017. An intercomparison of satellite-based daily evapotranspiration estimates under different eco-climatic regions in South Africa. *Remote Sens.* 9 (4), 307.
Malek, E., 1992. Night-time evapotranspiration vs. daytime and 24h evapotranspiration. J. Hydrol. 138 (1–2), 119–129.
Mazur, M.L.C., Wiley, M.J., Wilcox, D.A., 2014. Estimating evapotranspiration and groundwater flow from water-table fluctuations for a general wetland scenario. Ecohydrology 7 (2), 378–390.
McWhorter, D., and Sunada, D. (1977). "2_Campbell J." Ground-Water Hydrology and Hydraulics.
Michel, D., Jiménez, C., Miralles, D.G., Jung, M., Hirschi, M., Ershadi, A., Martens, B., McCabe, M.F., Fisher, J.B., Mu, Q., 2016. The WACMOS-ET project–Part 1: tower-scale evaluation of four remote-sensing-based evapotranspiration algorithms. *Hydrol. Earth Syst. Sci.* 20 (2), 803–822.
Miralles, D.G., Holmes, T.R.H., De Jeu, R.A.M., Gash, J.H., Meesters, A., Dolman, A.J., 2011. Global land-surface evaporation estimated from satellite-based observations. *Hydrol. Earth Syst. Sci.* 15 (2), 453–469.
Moore, P.A., Pypker, T.G., Waddington, J.M., 2013. Effect of long-term water table manipulation on peatland evapotranspiration. Agric. For. Meteorol. 106–119.
Moorhead, J.E., Marek, G.W., Gowda, P.H., Lin, X., Colaizzi, P.D., Evett, S.R., and Kutikoff, S. (2019). "Evaluation of evapotranspiration from eddy covariance using large weighing lysimeters." Agronomy, Multidisciplinary Digital Publishing Institute, 9(2), 99.
Mu, Q., Zhao, M., Running, S.W., 2011. Improvements to a MODIS global terrestrial evapotranspiration algorithm. Remote Sens. Environ. 1781–1800.
Nichols, W.D., 1994. Groundwater discharge by phreatophyte shrubs in the Great Basin as related to depth to groundwater. Water Resour. Res. 30 (12), 3265–3274.
Nosetto, M.D., Jobbagy, E., Jackson, R., Sznaider, G., 2009. Reciprocal influence of crops and shallow ground water in sandy landscapes of the Inland Pampas. Field Crop. Res. 113 (2), 138–148.
Novick, K.A., Oren, R., Stoy, P.C., Siqueira, M.B.S., Katul, G.G., 2009. Nocturnal evapotranspiration in eddy-covariance records from three co-located ecosystems in the Southeastern U.S.: Implications for annual fluxes. Agric. For. Meteorol. 149 (9), 1491–1504.
Ochoa, C.G., Fernald, A.G., Guldan, S.J., Shukla, M.K., 2007. Deep percolation and its effects on shallow groundwater level rise following flood irrigation. Trans. ASABE 50 (1), 73–82.
Peña-arancibia, J.L., Mainuddin, M., Kirby, J.M., Chiew, F.H.S., Mcvicar, T.R., Vaze, J., 2016. Assessing irrigated agriculture ' s surface water and groundwater consumption by combining satellite remote sensing and hydrologic modelling. Sci. Total Environ. 372–382.
Prathapar, S.A., Qureshi, A.S., 1999a. Modelling the effects of deficit irrigation on soil salinity, depth to water table and transpiration in semi-arid zones with monsoonal rains. Int. J. Water Resour. Dev. 15 (1–2), 141–159.
Prathapar, S.A., Qureshi, A.S., 1999b. Modelling the effects of deficit irrigation on soil salinity, depth to water table and transpiration in semi-arid zones with monsoonal rains. Int. J. Water Resour. Dev. 15 (1–2), 141–159.
Priestley, C., Taylor, R., 1972. On the assessment of surface heat flux and evaporation using large-scale parameters. Mon. Weather Rev. 100 (2), 81–92.
Rasmussen Mads Olander, S.ørensen, M. K, Wu, Yan, B., Qin, N., H, Sandholt, I., 2014. Regional-scale estimation of evapotranspiration for the North China Plain using MODIS data and the triangle-approach. Int. J. Appl. Earth Observ. Geoinf. 143–153.
Satchithanantham, S., Krahn, V., Sri Ranjan, R., Sager, S., 2014. Shallow groundwater uptake and irrigation water redistribution within the potato root zone. Agric. Water Manag. 132, 101–110.
Shah, N., Nachabe, M., Ross, M., 2007a. Extinction depth and evapotranspiration from ground water under selected land covers. Ground Water 45 (3), 329–338.
Shah, T., Burke, J., Villholth, K., Angelica, M., 2007b. Groundwater: a global assessment of scale and significance. Water Food Water Life.
Shankar, V., 2012. Effect of shallow groundwater table on the moisture depletion pattern in crop root zone. Int. J. Agric. Biosyst. Eng. 6 (12), 410–415.
Shouse, P.J., Goldberg, S., Skaggs, T.H., Soppe, R.W.O., Ayars, J.E., 2006. Effects of shallow groundwater management on the spatial and temporal variability of boron and salinity in an irrigated field. Vadose Zone J. 5 (1), 377–390.
Su, Z., 2002. The surface energy balance system (SEBS) for estimation of turbulent heat fluxes. Hydrol. Earth Syst. Sci. 6 (1), 85–100.
Sugita, M., Brutsaert, W., 1991. Daily evaporation over a region from lower boundary layer profiles measured with radiosondes. Water Resour. Res. 27 (5), 747–752.
Tang, R., Li, Z.L., Tang, B., 2010. An application of the Ts-VI triangle method with enhanced edges determination for evapotranspiration estimation from MODIS data in arid and semi-arid regions: Implementation and validation. In: Remote Sensing of Environment, 114. Elsevier Inc, pp. 540–551.
Tolk, J.A., Howell, T.A., Evett, S.R., 2006. Nighttime evapotranspiration from alfalfa and cotton in a semiarid climate. Agron. J. 98 (3), 730–736.
Ünlükara, A., Kurunç, A., Kesmez, G.D., Yurtseven, E., 2008. Growth and EVAPOTRANSPIration of Okra (Abelmoschus esculentus L.) as influenced by salinity of irrigation water. J. Irrig. Drain. Eng. 134 (April), 160–166.
Videla Mensegue, H., Degioanni, A., Cisneros, J., 2015. Estimating shallow water table contribution to soybean water use in Argentina. Eur. Sci. J. 11 (14), 23–40.
Wu, J., Kutzbach, L., Jager, D., Wille, C., Wilmking, M., 2010. Evapotranspiration dynamics in a boreal peatland and its impact on the water and energy balance. J. Geophys. Res.: Biogeosci. 115 (4), 1–18.
Xu, T., Guo, Z., Xia, Y., Ferreira, V.G., Liu, S., Wang, K., Yao, Y., Zhang, X., Zhao, C., 2019. Evaluation of twelve evapotranspiration products from machine learning, remote sensing and land surface models over conterminous United States. *J. Hydrol.* 578, 124105.
Xu, X., Zhang, Q., Li, Y., Li, X., 2016. Evaluating the influence of water table depth on transpiration of two vegetation communities in a lake floodplain wetland. Hydrol. Res. 47 (S1), 293–312.
Yang, J., Wan, S., Deng, W., Zhang, G., 2007. Water fluxes at a fluctuating water table and groundwater contributions to wheat water use in the lower Yellow River flood plain, China. Hydrol. Process. 21, 717–724.
Zhang, J.G., Xu, X.W., Lei, J.Q., Li, S.Y., Hill, R.L., Zhao, Y., 2013. The effects of soil salt crusts on soil evaporation and chemical changes in different ages of Taklimakan desert shelterbelts. J. Soil Sci. Plant Nutr. 13 (4), 1019–1028.
Zhang, Q., Xu, P., Chen, J., Qian, H., Qu, W., Liu, R., 2021. Evaluation of groundwater quality using an integrated approach of set pair analysis and variable fuzzy improved model with binary semantic analysis: A case study in Jiaokou Irrigation District, east of Guanzhong Basin, China. Sci. Total Environ. 767, 145247.
Zwart, S.J., Bastiaanssen, W.G.M., de Fraiture, C., Molden, D.J., 2010. WATPRO: a remote sensing based model for mapping water productivity of wheat. In: Agricultural Water Management, 97. Elsevier B.V,, pp. 1628–1636.